CRYSTALLIZATION IN CARBON NANOSTRUCTURES

EDOARDO MAININI AND ULISSE STEFANELLI

Abstract. We investigate ground state configurations for atomic potentials including both two- and three-body nearest-neighbor interaction terms. The aim is to prove that such potentials may describe crystallization in carbon nanostructures such as graphene, nanotubes, and fullerenes. We give conditions in order to prove that planar energy minimizers are necessarily honeycomb, namely graphene patches. Moreover, we provide an explicit formula for the ground state energy which exactly quantifies the lower-order surface energy contribution. This allows to give some description of the geometry of ground states. By recasting the minimization problem in three-space dimensions, we prove that ground states are necessarily nonplanar and, in particular, rolled-up structures like nanotubes are energetically favorable. Eventually, we check that the C_{20} and C_{60} fullerenes are strict local minimizers, hence stable.

1. Introduction

Crystallization is a fundamental issue in Materials Science. As such, it has attracted an immense deal of attention over the centuries from the physical, chemical, and technological viewpoint. In particular, the last decades have witnessed the discovery and applicative exploitation of carbon nanostructures. Among these *nanotubes* and *fullerenes* are three-dimensional carbon molecules showing unprecedented electro-mechanical properties which make them potentially useful in a wide variety of applications ranging from chemistry, to nano-electronics, to optics and mechanics. Even more recently, the production of isolated *graphene* sheets has lead to the attribution of the 2010 Nobel Prize in Physics to Geim & Novoselov. Lightweight and flexible yet extraordinarily strong, transparent and exceptionally conducting, graphene is presently believed to be one of the most promising materials available to mankind.

Form the microscopic viewpoint, crystallization is the result of interatomic interactions governed by quantum mechanics. At zero temperature, such interactions are expected to be ruled solely by the geometry of atoms configurations. From a mathematical standpoint, given a configuration of n atoms identified with their respective positions $\{x_1, \dots, x_n\}$ and a suitable configurational potential V, one considers the minimization problem $\min V(\{x_1, \dots, x_n\})$. *Crystallization* hence consists in proving the periodicity of ground-state configurations of V, that is, the emergence of an ideal crystal-lattice structure.

The focus of this paper is that of considering some simplified description of crystallization in carbon in the frame of classical potentials. In particular, we let $V = V_2 + V_3$ where V_2 is a short-ranged two-body interaction energy and V_3 is a three-body (*angular*) interaction potential. The two-body term V_2 favors atoms sitting at some reference distance from each other. On the other hand, the three-body potential V_3 is designed in order to take its minimum for bond angles of $2\pi/3$, thus corresponding to the classical covalent bonding behavior between sp^2-hybridized carbon orbitals.

2010 *Mathematics Subject Classification.* 82D25.
Key words and phrases. Ground state, graphene, nanotube, fullerene.

The first main result of this paper concerns the crystallization of a finite number of atoms in the plane: Under suitable conditions on the three-body potential, we show that planar minimizers of V are graphene patches, namely subsets of the regular hexagonal lattice (Theorem 6.1). Moreover, we provide the exact formula for the ground-state energy of n-atoms configurations (Corollary 6.6). The latter quantifies explicitly the surface energy due to the appearance of boundaries which in turn influences the global geometry of ground-state configurations.

Secondly, we move our discussion to three space dimensions where we prove that minimizers cannot be planar for large n (Theorem 7.1). In particular, our argument consists in checking that rolled-up structures like nanotubes are energetically competitive with respect to all planar configurations. Nanotubes and fullerenes are not three-dimensional ground states of V. On the other hand, we can prove that the fullerenes C_{20} and C_{60} are strict local minimizers, namely stable with respect to perturbations for a large class of potentials (Theorem 7.3).

Mathematical results on crystallization are by now quite classical in one space dimension. The reader is referred with no claim of completeness to [2, 3, 4, 15, 18, 25, 26, 27, 28, 36, 37, 38, 39] for a collection of results proving or disproving, under different choices for the energy, the minimization property of an equally spaced configuration of atoms and its stability with respect to perturbations. As for two space dimensions, for $V = V_2$ ground states have been firstly proved to be patches of the triangular lattice (hence crystalline) for some restricted class of potentials by Heitman & Radin [19, 29]. The considerably more involved case of Lennard-Jones-like potentials has been analyzed by Theil [34] in the *thermodynamic limit*, namely as the number of atoms of the configuration tends to infinity. This result has then been the extended to the case $V = V_2 + V_3$ by E & Li [10]. In particular, by assuming that V_2 is Lennard-Jones-like and V_3 presents sufficiently deep and narrow wells at $2\pi/3$ and $4\pi/3$, in [10] it is proved that in the thermodynamic limit the ground-state energy per atom converges to some specific value related to the hexagonal lattice.

Our analysis concerns the same class of functionals considered by E & Li [10], but in the specific case of *first-neighbors* interactions. Our tenet is that this choice appears to be well-suited for the description of covalent bonds in carbon, which are necessarily space localized. We do not take the thermodynamic limit but rather consider a finite and fixed number of atoms throughout. In particular, we give an explicit characterization of the ground state energy for all n-atoms configurations. In order to achieve this, we shall resort in assuming some qualification on the potential V_3, in the same spirit of Radin [29]. The choice of a suitable assumption frame is here quite delicate: We need to balance between the competing needs of ensuring crystallization in the plane and keeping enough surface tension for the emergence of three-dimensional structures. Indeed, our specific assumptions on V_3 are strong enough to entail that planar crystals are nothing but graphene patches. On the other hand, they are weak enough to permit three-dimensionality, see Section 7.

Let us mention that crystallization problems in three dimensions appear to be very challenging. In particular, we presently have no characterization of three-dimensional ground states for the energy V. In the case of two-body potentials V_2 rigorous crystallization results are still not available although *face-centered cubic* (FCC) and *hexagonally close-packed* (HCP) lattices are clearly the natural candidates to be ground states. We refer to [11] for some quantitative evidence in this direction. On the other hand, we shall mention the result announced by Flatley & Theil [12, 17] who argue that, by considering also three-body interactions $V = V_2 + V_3$ where V_3 favors $\pi/3$ bonds, the thermodynamic limit of the energy density of ground states corresponds to that of a suitably rescaled FCC lattice.

2. Energy

The understanding of the spatial arrangement of atoms into molecules by energy minimization is often referred to as *geometry optimization* [13]. In particular, the crystallization results recalled in the Introduction are examples of geometry optimization via classical potentials. Geometry optimization requires the specification of a suitable configurational energy. Many different model energies are in use, depending on the required level of detail as well as the dimension of the systems.

Ab initio configurational energies are obtained by quantum mechanical models. The chemical behavior of an atom or a molecule is governed by its electronic structure which in turn is described by the Schrödinger equation. In a time-independent non-relativistic frame, by assuming the standard *Born-Oppenheimer* approximation, nuclei are regarded as classical particles and Quantum Mechanics is involved for the description of the electrons only. Within this framework, by letting $\{x_1, \ldots, x_n\}$ indicate the nuclei positions, the energy can be written as $V(\{x_1, \ldots, x_n\}) := \min_\psi E(x_1, \ldots, x_n; \psi)$. Functional E is a quadratic form acting on the electronic wave function $\psi : (\mathbb{R}^3 \times \mathbb{Z}_2)^m \to \mathbb{C}$. The latter ψ depends on positions and spins (m being the number of electrons), it is normalized in L^2 and antisymmetric in the usual sense. In particuar, one has $E(x_1, \ldots, x_n; \psi) = \int_{(\mathbb{R}^3 \times \mathbb{Z}_2)^m} \psi^* H \psi$, where H is the electronic hamiltonian operator, parametrized by the nuclei positions $\{x_1, \ldots, x_n\}$, and accounting for Coulomb interactions and for the kinetic energy of electrons. The direct treatment of the above minimization of E is often precluded by the inherent number of dimensions, and the explicit form of V is generally not available. A variety of approximated quantum models including Density Functional Theory and Hartree-Fock-type models have been devised. See [22] for a general overview on all these issues. Still, for the treatment of large systems one often relies instead on the minimization of classical potential energies. In such case, V takes an explicit form, usually of Lennard-Jones type. More general potentials, accounting for multiple body interactions, can be used for capturing different atom bonding behaviors.

We consider here classical potentials minimization and focus on a minimal abstract frame capable of inducing graphene-like periodicity at zero temperature. Our choice of the energy (see below) is inspired by the many empirical potentials that have been set forth in order to describe interactions between carbon atoms, see the reference modeling papers [5, 6, 33] as well as the discussion in [13]. Let us emphasize the mathematical nature of our analysis, being beyond our purposes to target in detail the indeed quite rich physics and chemistry of carbon. A rigorous planar crystallization result, in the same spirit of [10, 19, 29, 34, 41], is our first goal.

We should also stress that this description regards the zero temperature situation and we recall that in some regimes two dimensional crystal ordering is prevented at positive temperature, see for instance [14].

We shall be considering two-dimensional particle systems. We will turn to 3D issues later in Section 7. Let C_n be a configuration of n identical *atoms* to be identified with their respective positions $x_1, \ldots, x_n \in \mathbb{R}^2$. The *energy* of such configuration will result from the contribution of both two-body and three-body interactions. In particular, given the atoms x_i and x_j we denote their distance by $\ell_{ij} = |x_i - x_j|$ and we associate to all ordered triples x_i, x_j, x_k the angle θ_{ijk} determined by the segments $x_i - x_j$ and $x_k - x_j$ (choose anti-clockwise orientation, for definiteness), see Figure 1.

The energy of the configuration will be given by the sum

$$V = \frac{1}{2} \sum_{i \neq j} V_2(\ell_{ij}) + \frac{1}{2} \sum_{A} V_3(\theta_{ijk}). \tag{1}$$

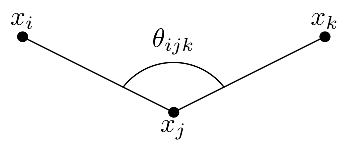

FIGURE 1. Notation for bonds and bond angles.

Here, the two-body interaction potential $V_2 : [0,\infty) \to [-1,\infty]$ is such that

$$V_2 = \infty \text{ on } [0,1), \quad V_2(1) = -1, \quad V_2(r) > -1 \text{ for } r > 1, \quad V_2(r) = 0 \text{ for } r \geq \sqrt{2}. \tag{2}$$

In particular, $r = 1$ represents the (normalized) carbon bond length and the constraint $V_2 = \infty$ on $[0,1)$ is usually referred to as *hard-interaction* assumption, see Figure 2. We say that x_i and x_j are *bonded* or that there is a (active) bond between x_i and x_j if $1 \leq \ell_{ij} < \sqrt{2}$. The set of (active) bonds forms a graph which we call *bond graph* and the fact that the functional V_2 vanishes for $r \geq \sqrt{2}$ entails that the graph is topologically planar: given a quadrilateral with all sides and one diagonal in $[1,\sqrt{2})$ the second diagonal is at least $\sqrt{2}$. In particular, we are restricting interactions to *nearest-neighbors* only. The factor $1/2$ in front of the two-body interaction part obviously reflects the fact that $\ell_{ij} = \ell_{ji}$, namely every bond is counted twice in the sum.

As for three-body interactions we let $V_3 = \mu v$ where $\mu > 0$, $v : [0,2\pi] \to [0,\infty)$ is Lipschitz continuous, v vanishes just in $2\pi/3$ and $4\pi/3$, and $v(2\pi{-}\theta) = v(\theta)$. We also require that v is convex on $[3\pi/5, 11\pi/15]$ and, for α in such interval, there holds $v(\alpha{+}2\pi/3) = v(\alpha)$. The set A in definition (1) corresponds to the triples (i,j,k) such that $1 \leq \ell_{ij}$, $\ell_{jk} < \sqrt{2}$, namely such that x_j is bonded to both x_i and x_k (in this case we say that θ_{ijk} is a (active) bond angle).

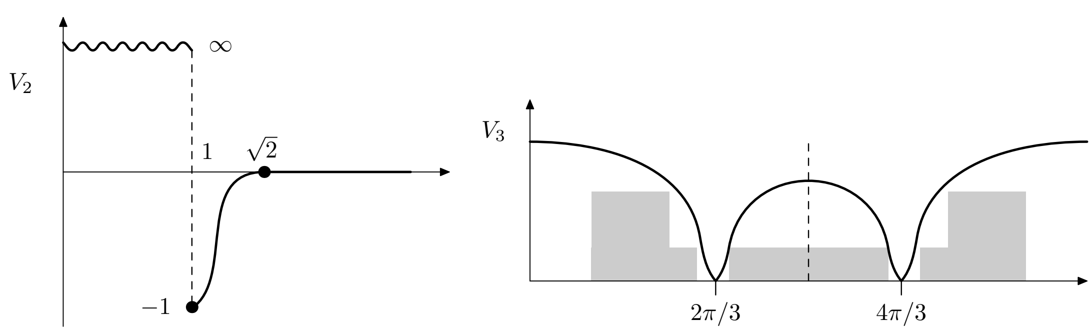

FIGURE 2. The potentials V_2 and V_3: Grey boxes illustrate (3)-(4).

The current form of V extracts the main common features of the empirical carbon potentials proposed in the literature: short-range pair-interactions and bond-angles penalization between nearest-neighbors, see [5, 6, 33].

The first main assumption of our theory is that the three-body interaction part of the energy does not degenerate in a prescribed quantitative fashion. In particular, we shall ask μ to be large enough in order to have

$$V_3 > 8 \ \text{ on } \ (\theta_{\min}, \pi/2], \tag{3}$$

$$V_3 > 3 \ \text{ on } \ (\theta_{\min}, 3\pi/5) \cup (5\pi/7, 9\pi/7) \cup (7\pi/5, 2\pi{-}\theta_{\min}), \tag{4}$$

see again Figure 2. In the latter $\theta_{\min} := 2\arcsin(1/(2\sqrt{2})) \approx 0.23\,\pi$ is the minimal angle which is attainable by a pair of active bonds. Note that some quantitative requirement of this sort is clearly necessary as the ground states for $\mu = 0$ could be patches of the triangular lattice [29, 34]. Hence, by progressively increasing μ, some symmetry-breaking bifurcation is to be expected (see Section 4). In particular, note that an analogous size assumption on μ is subsumed in [10] as well.

A second main assumption of our theory is that V_3 grows linearly out of optimal angles. In particular, we assume that μ is large enough in order to have

$$V'_{3,-}(2\pi/3) < -3/\pi \tag{5}$$

where $V'_{3,-}$ denotes the left derivative. This is reminiscent of Radin *soft-interaction* assumption from [29].

Before moving on we shall comment that assumptions (2)-(5) are chosen here for the sake of maximizing simplicity rather than generality. In particular, our theory remains valid under some weaker assumptions at the expense of some more elaborate arguments.

First, the two-body interaction potential V_2 can be generalized in order to avoid the hard-interaction restriction. In particular, we can assume that V_2 is large in a right neighborhood of 0 only (still keeping the unique minimizer $r = 1$), see Figure 3. Namely, we could ask for

$$V_2 \geq \frac{1}{\gamma} \ \text{ on } \ (0, 1-\gamma), \quad V_2(1) = -1, \quad V_2(r) > -1 \text{ for } r > 1, \quad V_2(r) = 0 \text{ for } r \geq 1+\gamma.$$

for some small $\gamma > 0$. Indeed, under the latter assumptions the statement in [10, Lemma 2.3] entails that all bonds in a ground state configuration have a minimal length which can be made arbitrarily close to one by letting γ small. In particular, for some critical γ we will have that the maximal number of bonds per ground state atom will be necessarily smaller than nine. As it will become apparent below, this is actually enough in order to run our analysis (see Lemma 3.1). We however prefer to stick to the case of hard interactions here for the sake of notational simplicity.

As for the assumptions on the three-body interaction part of the energy, one again could ask for some weaker conditions with respect to (3). For instance, in case V_2 vanishes on $[1+\varepsilon, \infty)$ for some $\varepsilon < \sqrt{2}-1$, assumption (3) can be weakened as follows

$$V_3 > 6 + [\varepsilon/0.15] \ \text{ on } \ (\theta_\varepsilon, \pi/2].$$

Here, $\theta_\varepsilon = 2\arcsin(1/(2+2\varepsilon))$ is now the minimal bond angle which is attainable by a pair of active bonds of length smaller than $1+\varepsilon$. In particular, $\theta_{\min} < \theta_\varepsilon < \pi/3$ and we have that $\theta_\varepsilon \to \pi/3$ as $\varepsilon \to 0$. Moreover, the symbol $[\cdot]$ stands for the right-continuous *integer part* function defined as $x \mapsto [x] = \max\{z \in \mathbb{Z} : z \leq x\}$. In particular, the above assumption gets weaker as $\varepsilon \to 0$. We however prefer to stick to assumption (3) in order to keep it independent from V_2 (that is, from ε). Concerning assumption (4), the values $3\pi/5$ and $5\pi/7$ are also not restrictive, one could take other numbers around $2\pi/3$. Notice that due to the structural assumptions on V_3, the condition $V_3(5\pi/7) \geq 3$ implies that also $V_3(3\pi/5) > 3$. Still we prefer to write assumption (4) giving emphasis to the pentagonal angle $3\pi/5$ which will play a role in the sequel.

Assumption (5) is needed in order to give a control on the energy of boundary atoms of the bond graph. However, we remark that we do not have the same requirement (the Radin soft-interaction assumption [29]) on the two-body potential. This is interesting because in the case $\mu = 0$, when we are reduced to a two-body interaction, finite crystallization is not known when omitting such requirement (see also [41]). In our result, the two-body term can have the general form of a short-ranged Lennard-Jones-like potential (see Figure 3).

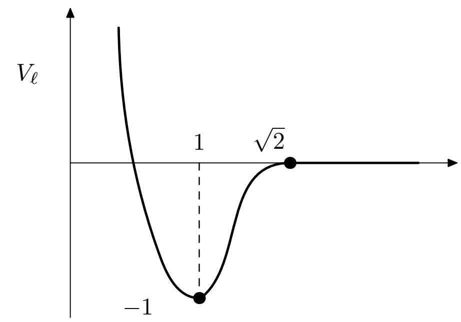

FIGURE 3. A more general choice for V_ℓ.

Let us mention that our assumptions on the potential V_3 are somehow intermediate between the two limiting situations depicted in Figure 4. The function v^s is singular at bond angles $2\pi/3$

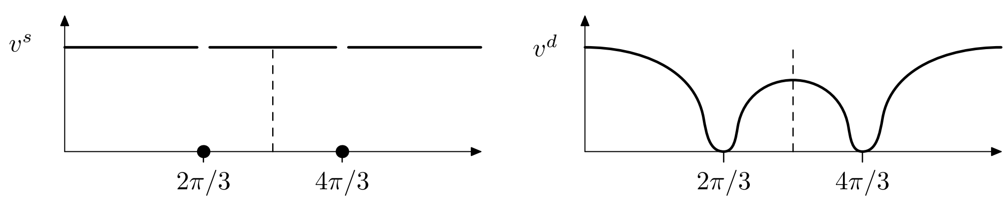

FIGURE 4. Two limiting examples for the potential V_3

and $4\pi/3$ whereas v^d is differentiable at those values. In particular, v^d recalls the *Stillinger-Weber* interaction potential given in some normalized form by $v^d(\theta) = (\cos\theta + 1/2)^2$ [32] and already mentioned in [10], see also [5, 6, 33]. By assuming $V_3 = \mu v^s$ (for $\mu > 0$ large) the planar crystallization problem would be drastically simplified as all bond angles at finite energy would be forced to $2\pi/3$. On the other hand, this would prevent from considering three-dimensional structures since three adjacent $2\pi/3$-bonds are necessarily planar. Namely, nanotubes and fullerenes would be out of reach of the theory. On the contrary, by letting $V_3 = \mu v^d$ three-dimensional ground states are even more favored (see Section 7 below) but planar crystallization is presently not known for finite-atoms configurations. We need here to balance between these two issues by assuming V_3 to be *sufficiently singular* at minima in order to entail planar crystallization but *not too singular* to allow for three-dimensionality.

In order to prove that planar ground-state configurations of V are subsets of the hexagonal lattice, we develop an induction argument on bond-graph layers which is reminiscent of that of [19, 29, 39]. In comparison with these papers, some extra care is here needed since the richer geometric structure of the hexagonal lattice calls for nontrivial adaptations. Our analysis departs from the former contributions in the control of the boundary energy. This is obtained by a novel argument based on the estimate of the ratio between two and three-bonded boundary vertices (Lemma 6.2). Moreover, the former results are here complemented in the direction of the discussion of the global geometry of ground-state configurations. In particular, we provide some explicit geometric construction in Section 4.

3. Geometric preliminaries

3.1. **Bond graph.** In the sequel, the notation $C_n = \{x_1, \ldots, x_n\}$ will refer to both the n-atoms configuration and its bond graph. In particular, we shall use equivalently the terms *atom* for *vertex* and *bond* for *edge*. Given a configuration, its energy is defined according to (1). In analogy with Quantum Mechanics, we will term *ground states* the global minimizers of the energy. If no ambiguity arises, for simplicity of notation we will denote the energy of a given configuration by V. Similarly, the number of bonds will be denoted by b. As the energy is clearly rotation and translation invariant, we shall tacitly assume in all of the following that statements are to be considered up to isometries. Note that, having fixed the number of atoms of a configuration, all ground states are necessarily contained in a ball of sufficiently large radius. In particular, the energy V is coercive, ground states exist, and the ground-state energy is negative.

A bond graph is connected if each two vertices are joinable through a simple path. Any simple cycle of the bond graph is a *polygon*. We term *acyclic* all bonds which do not belong to any simple cycle. Among these we distinguish between *flags* and *bridges*. We call *bridge* an acyclic bond which is contained in some simple path connecting two atoms which are included in two distinct cycles. On the other hand, we term *flags* all other acyclic bonds, see Figure 5. The bond graph would increase in the number of connected components by *removing* an acyclic

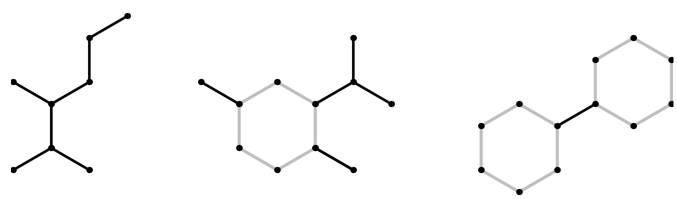

Figure 5. Examples of *flags* (bold in the first two) and a *bridge* (bold in the last picture).

bond. Here, we refer to *removal* of a bond as of considering *another* configuration where the bond subgraphs connected by the bond are shifted apart from each other in such a way that they are not bonded anymore. This can be done for any acyclic bond. We will denote by f (resp. g) the number of flags (resp. bridges). In what follows, we shall also refer to the *removal* of a given bonded atom x from a configuration. With this, we mean that we consider *another* configuration such that the atom x is relocated so far away that it has no active bonds. Notice that each flag can be considered as corresponding to a single atom: if we have f flags we can always *remove* exactly f atoms in order to deactivate the flag bonds.

Moving from energetic considerations, we shall record here some first elementary properties of the bond graph of ground states.

Lemma 3.1. *Ground-state atoms have at most three bonds.*

Proof. Note that each atom has at most eight bonds as $\theta_{\min} > 2\pi/9$. Assume now that the bonds at x_i are four or more. Hence, at least one of the bond angles centered in x_i is smaller than or equal to $\pi/2$. Then, assumption (3) ensures that by *removing* x_i the energy would strictly decrease. Indeed, no more of eight bonds are deactivated by this *removal* and the drop in V_3 is at least 8 by assumption (3). This contradicts the fact that the original configuration was a ground state. □

Lemma 3.2. *In a ground state all polygons have at least* 6 *edges and all convex polygons are hexagons.*

Proof. Assume that the bond graph of a ground state contains a simple pentagon. Then, at least one of the internal angles of the pentagon is smaller or equal to $3\pi/5$. Let this angle θ_{ijk} be centered at x_j. On the other hand, all bond angles are at least $\theta_{\min}$, and so is θ_{ijk}. Therefore, if we *remove* x_j we strictly decrease the energy because of assumption (4) (no more than three bonds are deactivated due to Lemma 3.1 and the drop in V_3 is more than 3). This contradicts the fact that the configuration is a ground state. The same argument excludes simple polygons with four or three edges. Suppose now to have a simple, convex polygon with more than 6 edges. Then, there is at least one bond angle which is greater than or equal to $5\pi/7$ and less than or equal to π. Therefore, due to assumption (4), by *removing* the corresponding atom we again strictly decrease the energy and contradict minimality. $\square$

3.2. **Honeycomb graph.** In the mathematical and chemical literature one can find a remarkable nonuniformity of notation and terminology when referring to hexagonal lattice structures. We hence start by clarifying here the objects we are going to deal with. We fix the *hexagonal lattice* to be the planar set $\{pa+qb+rc \, : \, p,q \in \mathbb{Z},\, r=0,1\}$ with $a=(\sqrt{3},0)$, $b=(\sqrt{3}/2,3/2)$, and $c=(\sqrt{3},1)$, see Figure 6, and term *honeycomb* the corresponding graph binding nearest neighbors. Note that the honeycomb graph is planar, connected, and all edges have unit length. We say that a configuration is *honeycomb* if it is a subset of the hexagonal lattice. Using the nonnegativity of V_3 and the minimality of V_2 for unit length bonds, it is clear that the elementary estimate

$$V \geq -b \tag{6}$$

holds, with equality if and only if the configuration is honeycomb. That is, in honeycomb configurations the energy is computed by simply counting the number of bonds.

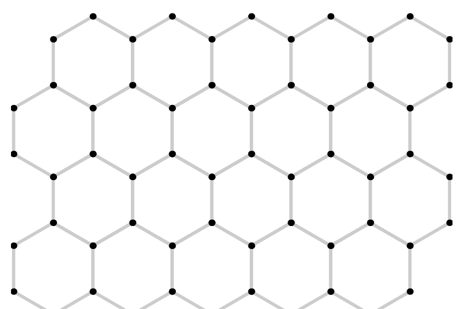

FIGURE 6. Honeycomb graph

We aim at proving that all ground states of the energy V are honeycomb (Theorem 6.1). A preliminary step in this direction is the following.

Proposition 3.3. *Let C_n with $1 \leq n \leq 6$ be a ground state. Then, C_n is honeycomb and its energy is $-(n-1)$ if $n \leq 5$ and -6 if $n=6$.*

Proof. Let $n \leq 5$. As we have the lower bound (6) and it is trivial to construct honeycomb configurations with n atoms and $n-1$ bonds, the result is achieved if we prove that the maximal number of bonds is $n-1$. Notice that for $n \leq 5$ each bond is a flag, otherwise there would be polygons with less than 6 edges, which is excluded by Lemma 3.2. Therefore, starting from a reference atom, if we add the other $n-1$ vertices one by one, each of them adds at most a flag.

If $n=6$, either we have (at most) five flags or we have a hexagon, and the energy of the regular hexagon with unit-length bonds is -6. $\square$

3.3. **Boundary energy.** Within the bond graph, we say that an atom is a *boundary atom* if it is not contained in the interior region of any simple cycle. Let us define the *energy of a boundary atom* x_i as $V^{(i)} = -r_i - s_i/2$ where r_i is the number of interior bonds at x_i (0 or 1), and s_i is the number of boundary bonds at x_i (1, 2 or 3). Taking into account Lemma 3.1, the possible values of the energy of a boundary atom of a ground state are x_i are $-1/2, -1, -3/2$, and -2. Given a n-atoms configuration C_n, we define its *bulk*, denoted by C_n^{bulk}, as the subconfiguration obtained by dropping all the boundary atoms. The bulk is therefore a $(n-d)$-atoms configuration, where d denotes the number of boundary vertices of C_n. We define V^{bulk} as the energy of C_n^{bulk}. Then, the energy of C_n can be seen as the sum of two contributions: V^{bulk} and V^{bnd}, where

$$V^{\text{bnd}} := V - V^{\text{bulk}}, \tag{7}$$

that is, V^{bnd} accounts for active bonds and bond angles of the configuration C_n that are not in C_n^{bulk}.

From the definition of V^{bnd}, we have

$$V^{\text{bnd}} \geq \sum_{i=1}^{d} V^{(i)} + \sum_{i} V_3(\theta_i) \geq \sum_{i=1}^{d} V^{(i)}, \tag{8}$$

where the second sum is extended to all the bond angles that contribute to V^{bnd}, (we stress that some of these may be adjacent to interior vertices). Notice that there is equality if the configuration is honeycomb: in this case indeed $-\sum_{i=1}^{d} V^{(i)}$ is reduced to the number of bonds in C_n^{bnd}.

In view of Lemma 3.2, we name *defect* any elementary polygon (that is, a simple cycle with no bonds in its interior region) in the bond graph which is not a hexagon (a polygon with six bonds). A configuration C_n is then said to be defect-free if all its elementary polygons are hexagons. Later on, we will see that ground states enjoy this property (see Proposition 6.7). Moreover, notice that in a honeycomb configuration at least a vertex of the hexagonal lattice is missing in the interior of a defect, and the minimal defect has 12 edges.

A distinguished role is also played by configurations with connected bond graph, no flags and no bridges ($f = g = 0$). The bond graph is then delimited by a simple cycle that we call the *boundary polygon*. For such graphs we adapt from [29] the following

Lemma 3.4. *Consider a ground state C_n. Suppose that C_n is connected and it has no flags nor bridges. Then,*

$$n - d \geq -4V + 6 - 5n, \tag{9}$$

and equality holds if and only if C_n is a defect-free honeycomb configuration.

Proof. Let h_j be the number of elementary j-gons in the bond graph and h be the total number of elementary polygons. We have

$$\sum_{j\geq 1} j h_j = 2b - d,$$

because by summing all bonds of elementary polygons, interior bonds are counted twice. From the latter and Lemma 3.2 we deduce

$$6h \leq 2b - d$$

where h is the number of elementary polygons, with equality if and only if all elementary polygons have six bonds. Combining this with the Euler formula $h + n = b + 1$ we get

$$n - d \geq 4b - 5n + 6. \tag{10}$$

Making use of the lower bound (6) we obtain the result. □

4. Daisies

As we will see in the next section, ground states are honeycomb, so that one would search for a honeycomb configuration attaining the maximal number of bonds. This can be heuristically restated as some minimality of the perimeter of the honeycomb configuration. This section is devoted to the explicit construction of some of these configurations, providing a reference energy value, namely

$$V = -[\beta(n)] \quad \text{where} \quad \beta(n) := 3n/2 - \sqrt{3n/2}.$$

By the specific geometry of the hexagonal lattice, it is quite natural to expect the leading term in the energy to be $-3n/2$ since each atom has three bonds and the bond angle contribution is zero. The additional lower-order correction $\sqrt{3n/2}$ is then the effect of boundary bonds.

We consider a very special class of subsets D_k of the hexagonal lattice with $n = 6k^2$ atoms which we term *daisies* because of their symmetry. Daisies are constructed in a recursive way. We define the daisy D_1 to be a hexagon and construct the daisy D_2 by externally attaching to all bonds of D_1 another hexagon. Then, the daisy D_3 is constructed by adding hexagons such that any boundary bond of D_2 has a new hexagon constructed on it. We continue constructing recursively for the daisy D_k, see Figure 4.1.

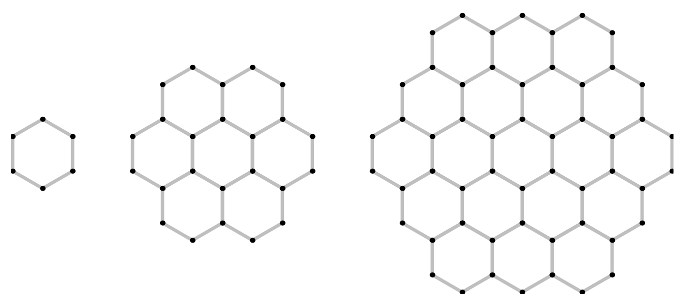

Figure 7. Daisies D_1, D_2, and D_3.

We start by computing the energy of a daisy. In particular, we have he following.

Proposition 4.1. *For all daisies we have $V = -[\beta(n)]$.*

Proof. Given the daisy D_k we denote by n_k the number of atoms, b_k the number of bonds, d_k the number of boundary atoms, $d_k^{(2)}$ the number of two-bonded boundary atoms, e_k the number of hexagons possessing boundary atoms, h_k the number of hexagons.

By referring directly to the construction of D_k, we can easily check that the following recursive relations hold true

$$d_k = 12 + d_{k-1}, \quad d_1 = 6, \tag{11}$$

$$n_k = n_{k-1} + d_k, \quad n_1 = 6, \tag{12}$$

$$b_k = b_{k-1} + 3d_{k-1}^{(2)} + 6, \quad b_1 = 6, \tag{13}$$

$$d_k^{(2)} = d_{k-1}^{(2)} + 6, \quad d_1^{(2)} = 6. \tag{14}$$

Moreover, note that $e_k = 6k-6$ for $k \geq 2$ and $e_1 = 1$. From relation (11) we have

$$d_k = 12k - 6.$$

Substituting the latter into relation (12) we find

$$n_k = n_{k-1}+12k-6 = 6 + \sum_{j=2}^{k}(12j-6) = 6 + 6(k+2)(k-1) - 6(k-1) = 6k^2,$$

and we observe that indeed $3n_k/2 = 9k^2$ is a square. On the other hand, we have that $e_k = d_k - d_k^{(2)}$ and $d_k^{(2)} = 6k$ (so that indeed $e_k = 6k - 6$). The total number of hexagons in D_k is hence

$$h_k = 1 + \sum_{j=2}^{k}(6j-6).$$

Eventually, from relation (13) we can now deduce that the number of bonds of the daisy D_k is

$$b_k = b_{k-1}+3d_{k-1}+6 = b_{k-1}+18(k-1)+6 = 6 + \sum_{j=1}^{k}(18j-12) = 9k^2-3k.$$

Now the assertion follows using (6), where equality is true for honeycomb configurations like daisies, as

$$V = -b_k = -9k^2 + 3k = -3n/2 + \sqrt{3n/2}$$

and the latter is integer. □

By inspecting the proof of the latter Lemma one realizes that indeed daisies can be constructed for $n = 6k^2$ only. We conjecture that, for such choice of n, daisies are the unique ground states of V. On the other hand, for $n \neq 6k^2$, the nonuniqueness of the ground states can be easily checked.

Before moving on let us mention that some specific highly-symmetric ground-state structure can be identified also in the case of simple two-body interaction potentials. For instance, by setting $\mu = 0$ in V and considering the two-body soft disk potential of Radin [29], we may find a symmetric ground state represented by an hexagon of edge k, constructed on the triangular lattice, see Figure 8. The value of the ground state energy for n-atoms configuration is obtained in [19, 29] as $-[3n - \sqrt{12n-3}]$ and symmetric states (daisies) in this context correspond indeed to integer values of $\sqrt{12n-3}$. In this respect, the reader is referred also to Yeung, Friesecke,

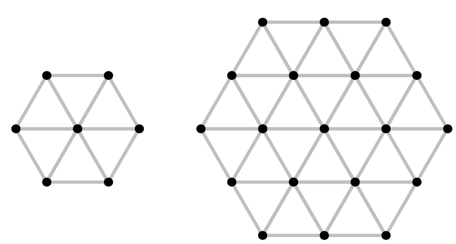

Figure 8. Symmetric ground states for $\mu = 0$.

& Schmidt [41] and Schmidt [31] for an analysis on the clustering of atoms and the emergence of a overall geometric shape as an effect of surface tension (still for the case $\mu = 0$). A discussion on the surface energy term in the thermodynamic limit $n \to \infty$ is in Theil [35] where it is proved that it can be expressed as a surface integral involving just the surface normal and the interaction potential. As mentioned in Section 2, the size of μ (which indeed modulates the relation between two- and three-body interactions) is clearly responsible for the symmetry pattern of ground states. In particular, by progressively increasing μ from zero, a symmetry-breaking phenomenon is expected to occur so that ground states turn from triangular to hexagonal patches. Some quantitative estimates in this direction are indeed available in dependence of n. For instance, by letting $n = 7$ one can argue that the honeycomb ground state lattice will surely be preferred to the triangular one (left in Figure 8) as soon as $\mu > 5/(18v(\pi/3)+3v(\pi))$. The appearance of intermediate geometries between the triangular and the honeycomb phases is to be expected.

5. Energy bound

The aim of this section is that of proving an upper energy estimate for ground states. In particular, we check for the following.

Proposition 5.1. *For all ground states C_n we have $V \le -[\beta(n)]$.*

Indeed, the latter inequality will be proved to be an equality and a characterization of ground states later on in Corollary 6.6. The proof of Proposition 5.1 consists in exhibiting C_n which realizes the inequality $V \le -[\beta(n)]$. This has been already done in Proposition 4.1 for daisies, namely for $n = 6k^2$. For all other values of n, we proceed by an explicit construction corresponding to some sort of *geometric interpolation* between the two closest daisies.

Proof. Proposition 4.1 proves the assertion for $n = 6k^2$. Let $6k^2 < n < 6(k+1)^2$ and define $m = n - 6k^2$ so that $1 \le m < 12k + 6$. We shall be computing the energy of a ground state with exactly $6k^2 + m$ atoms by progressively adding the m atoms to the daisy D_k. From here on we assume that $k \ge 2$ as the possibility of creating ground states with $n < 24$ atoms can be easily checked by hand (equivalently, by some simplified version of the arguments below).

Step 1: Construction of a $(6k^2+m)$*-atom configuration.* Let us first describe our construction: Starting from D_k we add a new atom x in the bond graph in such a way that it gets bonded to the uppermost among the rightmost atoms of D_k. Then, we add $x + (0, 1)$ as second atom. Subsequently, we progressively add atoms in by letting each new atom be bonded both with the latest added one and, possibly, with some atom of D_k. One can easily realize that this uniquely defines a procedure in order to (*clockwise*) add m atoms to D_k, see Figure 9.

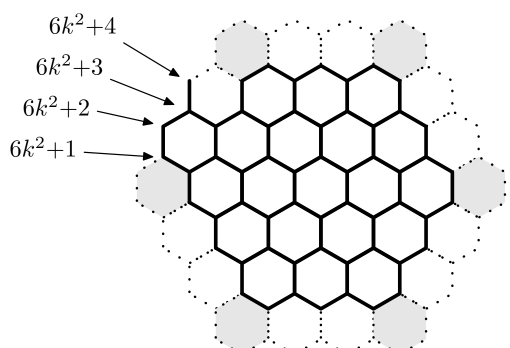

Figure 9. Construction of the $(6k^2+m)$-atom configuration for $k = 3$, $m = 4$.

Our aim is now to compute the number of new bonds which have been activated. By increasing m we progressively complete a connected series of new hexagons which correspond to the boundary hexagons of D_{k+1}. Initially, one needs three new atoms to form a new hexagon.

Then, one new hexagon is created every second newly added atom. This goes on for exactly $k-1$ hexagons so that the number of newly activated bonds is

$$d_k^m := \left\lceil \frac{3}{2}m - \frac{1}{2} \right\rceil \quad \text{for } 1 \le m \le 3+2(k-2) = 2k-1.$$

Then, the k-th hexagon of this series is a *corner* hexagon of D_{k+1}, in gray in Figure 9. This needs three new atoms to be completed, thus activating four new bonds. From there on, one completes a new hexagon (activating three new bonds) every two newly added atoms until $m = 4k$. As for the number of bonds, one has to sum up the newly activated bonds with those which were already active for $m = 2k-1$. In particular, we have

$$d_k^m = \left\lceil \frac{3}{2}(m-(2k-1)) - \frac{1}{2} \right\rceil + \left\lceil \frac{3}{2}(2k-1) - \frac{1}{2} \right\rceil = \left\lceil \frac{3}{2}m - 1 \right\rceil \quad \text{for } 2k \le m \le 4k.$$

This procedure can be restarted in correspondence to every *corner* hexagon of D_{k+1} and gives

$$d_k^m = \left\lceil \frac{3}{2}m - \frac{1}{2}q \right\rceil \quad \text{for } 2(q-1)k+q-2+2(q-2)^- \le m \le 2qk+q-2 \quad \text{and } q = 1, \dots, 6, \tag{15}$$

where we have used the notation $x^- = \max\{0, -x\}$ for the negative part. Note that, for $q = 6$, we reach exactly $m = 2qk+q-2 = 12k+4$. From there, we complete the last hexagon of D_{k+1} by achieving

$$d_k^{12k+5} = 18k + 4 \quad \text{and} \quad d_k^{12k+6} = 18k + 6.$$

Let us recall from Proposition 4.1 that the numbers b_k and d_k of bonds and boundary bonds, respectively, of D_k are $d_{k+1} = 12k + 6$ and $b_k = 9k^2 - 3k$. In particular, we have checked that by adding $m = d_{k+1} = 12k+6$ atoms to D_k one can reconstruct D_{k+1}. Moreover, the number of bonds of our $(6k^2+m)$-atom configuration is

$$b_{6k^2+m} = 9k^2 - 3k + d_k^m.$$

Step 2: The energy of the constructed configuration. In order to prove the result, making use of (6), we check that

$$-V = b_{6k^2+m} = 9k^2 - 3k + d_k^m \ge \left\lceil \frac{3}{2}(6k^2+m) - \sqrt{\frac{3}{2}(6k^2+m)} \right\rceil \quad \text{for } 1 \le m < 12k+6.$$

Equivalently, by using (15), we aim at proving that

$$\left\lceil -3k + \frac{3}{2}m - \frac{1}{2}q \right\rceil \ge \left\lceil \frac{3}{2}m - \sqrt{9k^2+\frac{3}{2}m} \right\rceil$$
$$\text{for } 2(q-1)k+q-2+2(q-2)^- \le m \le 2qk+q-2 \quad \text{and} \quad q = 1, \dots, 6,$$

that is

$$-3k + \frac{3}{2}m - \frac{1}{2}q \ge \left\lceil \frac{3}{2}m - \sqrt{9k^2+\frac{3}{2}m} \right\rceil \tag{16}$$
$$\text{for } 2(q-1)k+q-2+2(q-2)^- \le m \le 2qk+q-2 \quad \text{and} \quad q = 1, \dots, 6.$$

Note that the sequence

$$m \mapsto \left\lceil \frac{3}{2}m - \sqrt{9k^2+\frac{3}{2}m} \right\rceil - \frac{3}{2}m$$

attains its maximum for $m=2(q-1)k+q-2+2(q-2)^-$. By substituting the latter into (16) we reduce ourselves in proving

$$-3k+q \geq \left[\frac{3}{2}q - \sqrt{9k^2+3(q-1)k+\frac{3}{2}q-3+3(q-2)^-}\right] \quad \text{for} \quad q=1,\dots,6.$$

The latter corresponds to the following

$$1-3k+q > \frac{3}{2}q - \sqrt{9k^2+3(q-1)k+\frac{3}{2}q-3+3(q-2)^-} \quad \text{for} \quad q=1,\dots,6.$$

By taking the square on both sides, this is equivalent to

$$\frac{1}{4}q^2-2q-3(q-2)^- -2 < 3k \quad \text{for} \quad q=1,\dots,6,$$

which is clearly true as $k \geq 1$. □

6. Ground states are honeycomb

This section brings to our main crystallization result in the plane. In particular, we prove the following.

Theorem 6.1. *Ground states are honeycomb and connected.*

The most important tool for proving the latter is a boundary energy estimate. This requires assumptions (4) and (5) on the three-body potential V_3 and reads as follows.

Lemma 6.2. *Let $n \geq 6$. Let C_n be a ground state and assume it to be connected with no flags nor bridges. Then,*

$$V^{\rm bnd} \geq -[3d/2]+3. \tag{17}$$

Proof. Since no flags nor bridges are present, we can consider the boundary polygon of C_n. We denote by $\varepsilon \in [0,1]$ the ratio of its concave angles, by φ_i, $i=1,\dots,\varepsilon d$ such angles, and by α_i, $i=1,\dots(1-\varepsilon)d$ the remaining ones. Of course we have

$$\alpha(1-\varepsilon)d+\varphi\varepsilon d = \sum_{i=1}^{(1-\varepsilon)d}\alpha_i + \sum_{i=1}^{\varepsilon d}\varphi_i = \pi(d-2), \tag{18}$$

where α (resp. φ) denotes the mean value of the angles α_i (resp. φ_i). By the assumption (4) and the fact that C_n is a ground state we have that each convex angle α_i is not less than $3\pi/5$, so that $\alpha \geq 3\pi/5$, and similarly $\varphi \geq 9\pi/7$ (arguing as in Lemmas 3.1 and 3.2). Inserted into relation (18), these bounds entail

$$\varepsilon \leq \frac{7}{12}-\frac{35}{12d} < \frac{7}{12}. \tag{19}$$

Let us consider the energy estimate (8), also recalling that each atom has at most three bonds since C_n is a ground state, see Lemma 3.1. As the sum over the angles therein is made by nonnegative terms, we may reduce it to the ones involving just boundary atoms (thus neglecting the angles adjacent to interior vertices that contribute to $V^{\rm bnd}$). The energy of boundary vertices is -1 in correspondence of convex angles (no more then two bonds are there, otherwise an angle would be less than or equal to $\pi/2$) and it is not less than -2 otherwise. Summing up we write the basic estimate

$$V^{\rm bnd} \geq -(1-\varepsilon)d - 2\varepsilon d + \sum_{i=1}^{(1-\varepsilon)d} V_3(\alpha_i) + \sum_{\substack{i=1\\ i\in P}}^{\varepsilon d}\big(V_3(\varphi_i^1)+V_3(\varphi_i^2)\big) + \sum_{\substack{i=1\\ i\in Q}}^{\varepsilon d} V_3(\varphi_i), \tag{20}$$

where Q is the set of indices i for which the vertex in φ_i is two-bonded and P is the set of the remaining indices. Moreover, if the vertex corresponding to φ_i is three-bonded, that is if $i \in P$, we are denoting with $\varphi_i^1, \varphi_i^2 \in (3\pi/5, 5\pi/7)$ the two angles forming φ_i. Then, the structural assumptions on V_3 entail

$$\begin{aligned} &V_3(\varphi_i^1) + V_3(\varphi_i^2) \geq 2V_3(\varphi_i/2) \quad \text{for any } i \in P, \\ &V_3(\varphi_i) = V_3(\varphi_i - 2\pi/3) + V_3(2\pi/3) \geq 2V_3(\varphi_i/2) \quad \text{for any } i \in Q. \end{aligned}$$

Hence, still making use of the (local) convexity of V_3, from (20) and (18) we get

$$\begin{aligned} V^{\text{bnd}} &\geq -(1+\varepsilon)d + \sum_{i=1}^{(1-\varepsilon)d} V_3(\alpha_i) + \sum_{i=1}^{\varepsilon d} 2V_3(\varphi_i/2) \\ &\geq -(1+\varepsilon)d + (1-\varepsilon)dV_3(\alpha) + 2\varepsilon d V_3(\varphi/2) \\ &\geq -(1+\varepsilon)d + (1+\varepsilon)dV_3(\alpha_0(\varepsilon)), \end{aligned} \tag{21}$$

where

$$\alpha_0(\varepsilon) := \frac{\pi(d-2)}{(1+\varepsilon)d}.$$

We will obtain the lower bound for V^{bnd} by minimizing the right-hand side in (21) with respect to $\varepsilon \in [0, 7/12)$. The estimate $V^{\text{bnd}} \geq -[3d/2] + 3$ follows easily if $\varepsilon \leq ([d/2]-3)/d$, as in this case it is enough to consider the first term in the right hand side of (21) (notice also that $([d/2]-3)/d$ is nonnegative, because $d \geq 6$ from Lemma 3.2). Thus, in view of (19), and recalling that εd has to be integer, we may reduce to the case $\varepsilon \in [\varepsilon^*, 7/12]$, where $\varepsilon^* := ([d/2]-2)/d$. That is, we are left with

$$V^{\text{bnd}} \geq \min_{\varepsilon^* \leq \varepsilon \leq 7/12} -(1+\varepsilon)d + (1+\varepsilon)dV_3(\alpha_0(\varepsilon)). \tag{22}$$

We let $F(\varepsilon) := (1+\varepsilon)d\,(V_3(\alpha_0(\varepsilon)) - 1)$, on $[\varepsilon^*, 7/12]$. If the minimizer is attained at $\bar{\varepsilon}$ such that $\alpha_0(\bar{\varepsilon}) \leq 3\pi/5$, then it is enough to apply assumption (4), which immediately gives $F(\bar{\varepsilon}) \geq 0$ proving the result. So let us assume that the minimizer is attained at $\bar{\varepsilon} \in [\varepsilon^*, 7/12]$ such that $\alpha_0(\bar{\varepsilon}) > 3\pi/5$. In this case, since $\varepsilon \mapsto \alpha_0(\varepsilon)$ is decreasing we have that

$$\alpha_0(\varepsilon^*) > \alpha_0(\varepsilon) > \alpha_0(\bar{\varepsilon}) > 3\pi/5 \quad \text{for any } \varepsilon \in (\varepsilon^*, \bar{\varepsilon}). \tag{23}$$

Therefore, since V_3 is convex and decreasing on $(3\pi/5, 2\pi/3)$ we have

$$V_3(\alpha_0(\varepsilon^*)) \geq V_3(2\pi/3) + (\alpha_0(\varepsilon^*) - 2\pi/3)V'_{3\,-}(2\pi/3) \quad \text{and} \quad V'_3(\alpha_0(\varepsilon^*)) \leq V'_{3\,-}(2\pi/3). \tag{24}$$

Using the identity $(1+\varepsilon)\alpha'_0(\varepsilon) = -\alpha_0(\varepsilon)$, we compute the derivatives of F,

$$\frac{1}{d}F'(\varepsilon) = V_3(\alpha_0(\varepsilon)) - 1 - \alpha_0(\varepsilon)V'_3(\alpha_0(\varepsilon)) \quad \text{and} \quad \frac{1}{d}F''(\varepsilon) = -\alpha_0(\varepsilon)\alpha'_0(\varepsilon)V''_3(\alpha_0(\varepsilon)),$$

and we see that the estimates (24) entail

$$\begin{aligned} \frac{1}{d}F'(\varepsilon^*) &= V_3(\alpha_0(\varepsilon^*)) - 1 - \alpha_0(\varepsilon^*)V'_3(\alpha_0(\varepsilon^*)) \\ &\geq (\alpha_0(\varepsilon^*) - 2\pi/3)V'_{3\,-}(2\pi/3) - 1 - \alpha_0(\varepsilon^*)V'_{3\,-}(2\pi/3) \\ &= -1 - (2\pi/3)V'_{3\,-}(2\pi/3) > 0, \end{aligned}$$

where we made use of assumption (5) for the last inequality. On the other hand, since $\alpha'_0(\varepsilon) \leq 0$, from the monotonicity (23) and the convexity of V_3 on $(3\pi/5, 2\pi/3)$ we have $F''(\varepsilon) \geq 0$ on $[\varepsilon^*, \bar{\varepsilon}]$

which, together with $F'(\varepsilon^*) > 0$ entails that F is non decreasing on $[\varepsilon^*, \bar\varepsilon]$. As $\bar\varepsilon$ minimizes F we conclude that $\bar\varepsilon = \varepsilon^*$. The result eventually follows, since we have

$$\begin{aligned}
F(\varepsilon^*) &= (1+\varepsilon^*)d\ (V_3(\alpha_0(\varepsilon^*))-1)\\
&\geq ([3d/2]-2)\left((\alpha_0(\varepsilon^*)-2\pi/3)V'_{3\,-}(2\pi/3)-1\right)\\
&\geq ([3d/2]-2)\left(\frac{\pi d-2\pi-2\pi[3d/2]/3+4\pi/3}{[3d/2]-2}V'_{3\,-}(2\pi/3)-1\right)\\
&\geq -[3d/2]+2-\frac{\pi}{3}V'_{3\,-}(2\pi/3)\\
&> -[3d/2]+3,
\end{aligned} \tag{25}$$

where we used again relations (24) and assumption (5). □

An immediate corollary of the boundary energy estimate of Lemma 6.2 reads as follows.

Corollary 6.3. *Let $n \geq 6$. Let the ground state C_n be connected and have no flags nor bridges. If $C_n^{\rm bulk}$ is honeycomb and C_n is not, then inequality* (17) *is strict. Equality in* (17) *implies that d is even.*

Proof. By following the proof of Lemma 6.2 we shall identify the cases of equality in all the inequalities. Assuming that $C_n^{\rm bulk}$ is honeycomb, if the length of some bond of C_n is not 1, we have strict inequalities in (8) and (20). We also have a strict inequality in (20) if some of the angles that we neglected therein (the ones adjacent to interior vertices that contribute to $V^{\rm bnd}$) is different from $2\pi/3$ or $4\pi/3$. Moreover, the only case of possible equality in (21) corresponds to $\varepsilon = ([d/2]-3)/d$, since the proof of Lemma 6.2 shows that all other cases entail the strict inequality. If $\alpha_0(([d/2]-3)/d)$ is not equal to $2\pi/3$ (which is the case if d is odd), the term involving V_3 in the right-hand side of (21) gives a positive contribution, so that the inequality is strict. Summing up, if $C_n^{\rm bulk}$ is already known to be honeycomb the equality $V^{\rm bnd} = -[3d/2]+3$ implies that the entire configuration C_n is honeycomb as well. □

Before proceeding with the proof Theorem 6.1, we state some useful, elementary inequalities for the function $\beta(n) = 3n/2 - \sqrt{3n/2}$.

Lemma 6.4. *Let $n \geq 1$. Then $[\beta(n-1)] + 1 \leq [\beta(n)]$ and $[\beta(n-1)] + 3 \geq [\beta(n+1)]$.*

Proof. By definition of β, the inequality $\beta(n-1)+1 \leq \beta(n)$ (which implies the desired one) is equivalent to $\sqrt{3n/2} - 3/2 \leq \sqrt{3n/2-3/2}$. The latter is clearly true for any positive integer. Analogously, the inequality $\beta(n-1)+3 \geq \beta(n+1)$ is equivalent to $\sqrt{3n/2-3/2} \leq \sqrt{3n/2+3/2}$ which again can be directly checked. □

Lemma 6.5. *Let $n \geq 12$ and $6 \leq m, n-m \leq n$. Then,*

$$[\beta(m)] + [\beta(n-m)] + 1 \leq [\beta(n)] \tag{26}$$

and the equality holds if and only if $n = 12$ and $m = 6$.

Proof. Note that β is increasing and strictly convex. In particular, it is immediate to check that $m \mapsto \beta(m) + \beta(n-m)$ attains its maximum over the given range for $m = 6$ or $m = n-6$. Hence, we have that

$$\begin{aligned}
[\beta(m)] + [\beta(n-m)] + 1 &\leq \beta(m) + \beta(n-m) + 1 \leq \beta(6) + \beta(n-6) + 1\\
&= 6 + \frac{3}{2}(n-6) - \sqrt{\frac{3}{2}(n-6)} + 1.
\end{aligned}$$

For all n large enough, the above right-hand side is strictly smaller than $\beta(n)-1$ which in turn is controlled by $[\beta(n)]$. In particular, it is easily proved that

$$6+\frac{3}{2}(n-6)-\sqrt{\frac{3}{2}(n-6)}+1<\beta(n)-1=\frac{3}{2}n-\sqrt{\frac{3}{2}n}-1$$

whenever $n \geq 17$, so that the assertion follows. The remaining cases $n=12,\dots,16$ can be checked directly. □

Proof of Theorem 6.1. We aim at proving the following claim: If C_n is a ground state then it is honeycomb, connected, and $V=-[\beta(n)]$. In order to check this we proceed by induction on n. For $n \leq 6$ the claim follows from Proposition 3.3. Let us assume that it holds for all ground states C_m with $m<n$ and prove it for n.

Step 1: Nonhoneycomb C_n with flags. Suppose that the ground state C_n is not honeycomb and has a flag. If C_{n-1} obtained by cutting the flag is not honeycomb, by induction its energy is strictly greater than $-[\beta(n-1)]$, therefore

$$V>-[\beta(n-1)]-1 \tag{27}$$

since each flag decreases the energy at most by 1. By combining the latter with the inequality $[\beta(n-1)]+1 \leq [\beta(n)]$ from Lemma 6.4 we obtain that $V>-[\beta(n)]$. This contradicts the fact that C_n is a ground state by Proposition 5.1. If C_{n-1} is honeycomb, then the considered flag is not of unit length or creates an angle which is not $2\pi/3$ nor $4\pi/3$ (otherwise C_n would have been honeycomb itself). By the inductive assumption the energy of C_{n-1} is greater than or equal to $-[\beta(n-1)]$, and in this case the contribution of the flag to the energy is strictly greater than -1, thus (27) holds and we conclude that $V>-[\beta(n)]$ in the same way, again contradicting the fact that C_n is a ground state.

Step 2: Nonhoneycomb C_n with bridges. Suppose that the ground state C_n is not honeycomb and has a bridge. Consider the two subconfigurations C_m and C_{n-m} which are connected by the bridge. If both C_m and C_{n-m} are honeycomb and C_n is not, then the bridge is not of unit length or creates an angle which is not $2\pi/3$ nor $4\pi/3$ (otherwise C_n would have been honeycomb itself), so that its contribution to the energy is strictly greater than -1. By the induction assumption we get

$$V>-[\beta(m)]-[\beta(n-m)]-1 \geq -[\beta(n)],$$

where the latter inequality follows from Lemma 6.5. This contradicts the fact that C_n is a ground state by Proposition 5.1. In case one out of C_m or C_{n-m} is not honeycomb, the sum of their energies is strictly greater than $-[\beta(m)]-[\beta(n-m)]$ by induction. Since the bridge contribution to the energy is in general greater than or equal to -1, we still get $V>-[\beta(m)]-[\beta(n-m)]-1$ and we conclude $V>-[\beta(n)]$ with Lemma 6.5. Hence, C_n is not a ground state, a contradiction.

Step 3: C_n not connected. If the ground state C_n has two or more connected components, by arguing similarly as above we use the induction assumption and obtain an inequality of the form $V \geq -[\beta(m)]-[\beta(n-m)]$. This still implies $V>-[\beta(n)]$ by using Lemma 6.5 contradicting the fact that C_n is a ground state.

Step 4. Nonhoneycomb and connected C_n with no flags nor bridges. Owing to Steps 1-3, we are left with the most important case, a connected ground state C_n with no flags nor bridges. Suppose that C_n is not honeycomb. Then, either the bulk is not honeycomb itself, or it is still honeycomb. In the first case, by induction

$$V^{\text{bulk}}>-\left[\frac{3}{2}(n-d)-\sqrt{\frac{3}{2}(n-d)}\right]. \tag{28}$$

In the second case, we have

$$V^{\mathrm{bnd}} > -[3d/2] + 3, \tag{29}$$

as a consequence of Corollary 6.3. By using relations (7) and (17), and recalling that by induction we always have $V^{\mathrm{bulk}} \geq -[\beta(n{-}d)]$, in both cases we get

$$V > -\left[\frac{3}{2}(n{-}d) - \sqrt{\frac{3}{2}(n{-}d)}\right] - [3d/2] + 3 \geq -\left[\frac{3}{2}n - \sqrt{\frac{3}{2}(n{-}d)}\right] + 3. \tag{30}$$

Since the right-hand side is integer, the strict inequality implies

$$-([-V]+1) \geq -\frac{3}{2}n + \sqrt{\frac{3}{2}(n{-}d)} + 3. \tag{31}$$

On the other hand, as C_n is not honeycomb we have from (6) that $V > -b$. We recall that V is negative (otherwise it is obvious that $V > -[\beta(n)]$, hence C_n is not a ground state). Since b is integer, $-V < b$ implies $[-V] \leq b - 1$, which, together with relation (10), entails

$$4[-V] \leq 4b - 4 \leq 6n - d - 6 - 4.$$

This is equivalent to

$$n - d \geq 4([-V]+1) - 5n + 6. \tag{32}$$

By using relation (32) into inequality (31) we get

$$-([-V]+1) \geq -\frac{3}{2}n + \sqrt{\frac{3}{2}(4([-V]+1) - 5n + 6)} + 3.$$

As the function $x \mapsto x + 3n/2 - 3 - \sqrt{3(-4x+6-5n)/2}$ is nondecreasing and vanishes for $x = -\beta(n)$, the above inequality implies

$$-([-V]+1) \geq -\frac{3}{2}n + \sqrt{\frac{3}{2}n},$$

but now the left hand side is integer, therefore

$$V > -([-V]+1) \geq -\left[\frac{3}{2}n - \sqrt{\frac{3}{2}n}\right].$$

That is, $V > -[\beta(n)]$ contradicting the fact that C_n is a ground state.

Step 5: Energy equality. We have shown that C_n is honeycomb and connected. Since we already know that $V \leq -[\beta(n)]$ by Proposition 5.1, what we are left to prove is the opposite inequality.

As C_n is honeycomb, in case it has a flag, by using induction and the fact that a flag decreases the energy at most by 1, we have that $V \geq -[\beta(n{-}1)] - 1$. Then, the lower bound $V \geq -[\beta(n)]$ follows by Lemma 6.4. If C_n has two subconfigurations that are connected by a bridge (or that are two distinct connected components), by induction we find $V \geq -[\beta(n{-}m)] - [\beta(m)] - 1$, where $n - m, m$ are the numbers of atoms of the subconfigurations. Then, the lower bound $V \geq -[\beta(n)]$ follows by applying Lemma 6.5. The case of more connected components is reduced to the previous one.

Finally, if C_n has a single connected component, no flags and no bridges, by using (7), induction, and Lemma 6.2 we get that

$$V \geq -[\beta(n{-}d)] - [3d/2] + 3 \geq -\left[\frac{3}{2}n - \sqrt{\frac{3}{2}(n{-}d)}\right] + 3.$$

Then, using relation (9) we find

$$V \geq -\left[\frac{3}{2}\,n - \sqrt{\frac{3}{2}\,(-4V{-}5n{+}6)}\right] + 3 \geq -\frac{3}{2}\,n + \sqrt{\frac{3}{2}\,(-4V{-}5n{+}6)} + 3.$$

By following the final part of Step 4, the above inequality implies $V \geq -\beta(n)$, upon noting that the function $x \mapsto x + 3n/2 - 3 - \sqrt{3(-4x{+}6{-}5n)/2}$ is nondecreasing and vanishing for $x = -\beta(n)$. But $V = -b$ since C_n is honeycomb. In particular V is integer and the assertion $V \geq -[\beta(n)]$ follows. □

By considering the proof of Theorem 6.1, we are in the position of stating a characterization of ground states in terms of their energy. In particular, we have the following.

Corollary 6.6. *Ground states are characterized by the equality* $V = -[\beta(n)]$.

By using Corollary 6.6 one immediately obtains that all daisies as well as all configurations constructed in the proof of Proposition 5.1 are ground states. Moreover, one can check that the only ground state with a bridge is the right-most configuration in Figure 5. Indeed, let a ground state contain a bridge connecting two subsets of m and $n{-}m$ atoms each. By Theorem 6.1, the configuration is honeycomb. From minimality we necessarily have that m and n realize the equality in relation (26). Hence, by Lemma 6.5 we have that $n = 2m = 12$.

We conclude the geometric characterization of ground states by showing that they have no defects. In the following lemma, given a honeycomb configuration with some defect, we name *sink* each vertex of the hexagonal lattice which is missing in the interior of the defect.

Proposition 6.7. *All ground states are defect-free.*

Proof. It is enough to consider ground states without flags, because if a ground state C_n has f flags, the $(n{-}f)$-atoms configuration obtained by removing all flags is still a ground state. Indeed, suppose that this is not the case. Then, since the energy drop due to each flag is at most 1, we have $V > -[\beta(n{-}f)] - f$. Hence, Lemma 6.4 yields $V > -[\beta(n)]$, a contradiction to minimality due to Corollary 6.6.

Suppose there is a single sink in a honeycomb configuration. This corresponds to a twelve edges defect. By filling the sink one activates three bonds. So it is enough to take a two-bonded boundary atom (which does always exist) and place it at the sink and the energy decreases. This shows that a configuration with only a single sink is not a ground state.

Then, we use induction on the number m of sinks. Assume that any honeycomb configuration with a defect containing at most $m{-}1$ sinks, $m > 1$, is not a ground state and let by contradiction C_{n-1} be a ground state (hence honeycomb) with a defect containing m sinks. We shall be distinguishing two cases. At first, suppose that in the defect with m sinks there is a sink at distance 1 from three distinct vertices of the defect. In this case it is again enough to move a two-bonded boundary atom and place it in correspondence of that sink in order to decrease the energy and contradict minimality. On the other hand, suppose that in the defect with m sinks, there is no sink at distance 1 from three distinct vertices of the defect. Since the defect is a closed polygon, it necessarily possess at least two consecutive interior angles of $2\pi/3$. This means that three consecutive edges of the defect belong to the same unit hexagon. Therefore, placing two atoms in the two sinks completing the hexagon would mean to activate three new bonds: we let C_{n+1} be this new configuration. Since C_{n+1} has $m-2$ sinks, by induction there holds

$$-[\beta(n{+}1)] < V(C_{n+1}) = V(C_{n-1}) - 3.$$

Combining this with the second inequality of Lemma 6.4, we deduce $V(C_{n-1}) > -[\beta(n-1)]$, a contradiction. □

7. Nonplanar ground states

The energy V has a clear *planar* nature as it consists of two- and three-body interaction terms only. On the other hand, the very definition of V makes sense also in three-dimensional space. In this section, we investigate some consequence of assuming V to be defined on configurations of atoms in $\mathbb{R}^3$. The aim is that of relating V to the description of some specific three-dimensional allotropes of carbon: fullerenes and nanotubes. We shall not attempt to review on the complex phenomenology of these molecules, let us just record from Kroto [21] that fullerenes are clusters of carbon atoms forming a so-called *closed cage* composed of twelve pentagons and an unrestricted number of hexagons. Among these, the most common is C_{60} which consists of twelve planar pentagons and twenty planar hexagons (*soccer ball*). The existence of fullerenes has been theoretically speculated since the 70s. Their experimental discovery by Curl, Kroto, & Smalley in 1985 lead to the 1996 Nobel Prize in Chemistry.

Nanotubes are cylindrical structures with atom-thick carbon walls. Ideally, nanotubes can be visualized as the result of the roll-up of a graphene strip (sometimes referred to as a *graphene nanoribbon*). In particular, given the characteristic *chiral* vector (p, q), the roll-up is such that the atom x gets identified with $x + pa + qb$. Nanotubes are called *armchair* for $p = q$, *zigzag* for $p = 0$, and *chiral* in all other cases, see Figure 10. Carbon nanotubes (either single- or multi-

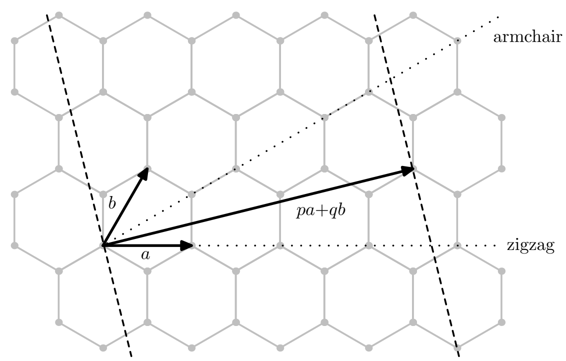

Figure 10. Rolling-up of nanotubes from a graphene sheet.

walled) show remarkable electro-mechanical properties and are believed to be possibly playing a major technological role in the near future. The reader is referred to [1, 40] and the references therein for an account on atomistic-based description of the mechanics of carbon nanotubes.

Our functional frame, although extremely simplified, describes to some extent the emergence of these three-dimensional structures. Of course nonplanar ground states exist. Indeed, whenever a planar ground state exhibits a flag (and already for $n = 4$) one can find a *nonplanar* configuration realizing exactly the same energy by simply tilting the flag out of the plane. On the other hand, one may then wonder whether by dropping the planarity constraint one could realize a strictly smaller energy. In other words, if three-dimensional ground states happen to be necessarily nonplanar. Leaving this issue open for small n (for $n = 6$, even in three space dimensions, the regular hexagon, the *benzene* cycle, is the only ground state), the first result of this section proves that ground states are necessarily nonplanar for large n. This evidence is reminiscent of the applicative difficulty of realizing two-dimensional crystallization in practice. The reader is also referred to GRIVOPOULOS [16] for an argument against honeycomb crystallization for an infinite configuration interacting via Lennard-Jones-like potentials in two-dimensional space. Before moving on let us mention that the results of this section do not require assumption (5) but are rather valid in some more generality. In particular, we can allow here some differentiable potential V_3, possibly of the form $V_3 = \mu v^d$, see Figure 4.

Theorem 7.1. *There exists no planar ground state for large n.*

Proof. We aim at exhibiting a three-dimensional configuration whose energy is strictly less than $-[3n/2-\sqrt{3n/2}]$ by rolling-up a sufficiently big planar hexagonal configuration. In doing so, we pay some three-body energy as we are forced to leave the optimal bond angles $2\pi/3$ but we are gaining on the two-body interaction term as we are activating extra bonds by rolling-up. We shall show that the overall balance is favorable.

Let us focus first on the case of $n = 6k^2$. We shall consider the daisy D_k to be ideally embedded in an infinite hexagonal lattice and roll it up in an *armchair* nanotube defined by the vector (k, k). By resorting to either the so-called *conventional* (or *rolled-up*) model [9] or the *polyhedral* model for nanotubes [7], we have that the bond angles (depending on the model either all of them or some of them, the others being $2\pi/3$) behave like

$$\theta = 2\pi/3 + \mathrm{O}(1/k^2) \quad \text{as} \quad k \to \infty.$$

Hence, the energy loss in the three-body interaction term fulfills

$$\frac{1}{2}\sum_{A} V_3(\theta_{ijk}) \sim ck^2 V_3(2\pi/3 + \mathrm{O}(1/k^2)) = \mathrm{O}(1) \quad \text{as} \quad k \to \infty.$$

On the other hand, the gain in the two-body energy part is exactly $-k$ for it amounts to a fixed finite number of newly activated bonds. In particular, one can compute that

$$\begin{aligned} V_{\text{rolled-up}} &= -9k^2 + 3k - k + \mathrm{O}(1) = -3n/2 + \sqrt{2n/3} + \mathrm{O}(1) \\ &< -3n/2 + \sqrt{3n/2} = V_{\text{planar}} \qquad \text{for } n \text{ large.} \end{aligned} \tag{33}$$

Hence, it is enough to take a sufficiently large $n = 6k^2$ in order to have that the rolled-up daisy is favorable with respect to the planar one.

The argument for general n is analogous, just starting from a ground state which is intermediate between daisies, in the same spirit as in the proof of Proposition 5.1. □

Before moving on we shall comment that the same argument of Theorem 7.1 applies to the behavior of a nanotubes as well. Indeed, assume to be given a indefinitely long graphene strip cut along some orthogonal direction to a given chiral vector (p, q), see the dashed lines in Figure 10. Arguing as in the proof of Theorem 7.1 we clearly have that, by letting $p+q$ be large enough, one can find a critical strip width starting from which it is energetically favorable to roll-up the strip into a nanotube. The emergence of such a critical width somehow relates to the fact that, depending on the chiral direction, some minimal nanotube diameter is observed. Moreover, the energy loss by rolling-up increases with the strip width. This represents the evidence that larger nanotubes show enhanced stability.

An interesting feature of the functional V is its capability of predict the *aspect ratio* of carbon nanotubes, as suggested by MIELKE [24]. In particular, we can check that, by progressively adding atoms to a nanotube, its diameter remains constant and its length scales with the number of atoms. This provides an illustration of the fact that carbon nanotubes are presently grown to lengths which are up to 10^8 times the diameter. This corresponds to the fact that, by progressively increasing n, namely adding atoms to a carbon nanotube, the functional V drives the structure to maintain a constant diameter and to grow at the ends. We record this fact in the following statement.

Proposition 7.2. *The length of a nanotube scales like n.*

Proof. For the sake of definiteness, let us focus on zigzag nanotubes. Other geometries can be treated analogously. Assume to be given a *rectangular* graphene patch consisting in λ rows of w hexagons, piled up in a zigzag configuration (that is $(p,q) = (w{+}1, 0)$). The patch can be conveniently rolled up in direction $(1,0)$ as soon as its *width* w is large enough (and regardless of its *length* λ). By rolling up the patch one activates new bonds so that the energy drops, to first order, by the quantity $-\lambda + 1$. On the other hand, the roll-up causes the angles to deviate from the optimal angle $2\pi/3$ by some quantity of the order of w^{-2} (recall that w is large). Correspondingly, the energy loss per angle bond is proportional to w^{-2} (see the proof of Theorem 7.1) and, by summing up for the n atoms, we get that the loss in the three-body interaction contribution scales like nw^{-2}. As n is proportional to $w\lambda$ (again to first order), we have checked that the roll-up entails an energy change of the order of $1 - \lambda + c\lambda^2 n^{-1}$. By minimizing the latter with respect to λ we identify the optimal scalings as $\lambda \sim n$ and w is constant. □

Let us conclude this discussion by explicitly remarking that nanotubes are not ground states for large n. Indeed, the argument of Proposition 7.2 entails that the energy of a nanotube scales like $-3n/2 + \mathrm{O}(n)$. The factor $-3n/2$ follows since each atom in the nanotube has three bonds. The $\mathrm{O}(n)$ correction takes into account the fact that bond angles are non-optimal. Note that, by increasing n bond angles do not change since the diameter of the nanotube is constant from Proposition 7.2. On the other hand, the computation in (33) shows that the energy of a rolled-up daisy behaves like $-3n/2 + \mathrm{O}(\sqrt{n})$, as well as the energy of the daisy itself. By increasing n the *radius* of the rolled-up daisy increases and its bond angles get closer to the optimal $2\pi/3$. This is reflected in the different scaling of the correction term. Eventually, for large n it is better to roll-up a daisy instead of a rectangular patch.

7.1. **Stability of fullerenes.** From the applicative viewpoint, the *stability* of carbon structures and, particularly, of fullerenes bears of course a crucial relevance. The aim of this section is to present a rigorous stability proof within our variational frame. In particular, we prove that the two fullerenes C_{20} (unsaturated *dodecahedrane*, a regular dodecahedron) and C_{60} (the smallest fullerene presenting isolated pentagons) are strict local minimizers for the energy provided the three-body interaction part is decreasing and strictly convex around $3\pi/5$.

Theorem 7.3. *Let V_3 decreasing and convex in a neighborhood of $3\pi/5$. Then, C_{20} and C_{60} are strict local minimizers, hence stable.*

Let us comment that the monotonicity and convexity of V_3 follows for the Stillinger-Weber potential (see Section 2) and it is completely independent of the size of μ. In particular, the validity of Theorem 7.3 is independent from the actual form of the two-body interaction term V_2 which can be arbitrarily chosen, provided that attains its minimum in 1. On the other hand, let us remark that under assumption (4), no fullerene is a ground state as the energy decreases by removing the five vertices of a pentagon.

Proof of Theorem 7.3. Let us develop the proof for $\mathrm{C}_{60} = \{x_1, \ldots, x_{60}\}$, the argument for C_{20} being analogous. Let $\{\tilde{x}_1, \ldots, \tilde{x}_{60}\}$ be some small perturbation of C_{60}. We shall prove that indeed, $\tilde{V} > V$. The perturbed configuration has exactly twelve 5-cycles and twenty 6-cycles.

Within the bond angles of the perturbed configuration we shall distinguish between *internal* angles of 5-cycles and those of 6-cycles. In particular, we indicate π_j^k the angles of 5-cycles ($j = 1, \ldots, 5, k = 1, \ldots, 12$) and by h_j^k those of 6-cycles ($j = 1, \ldots, 6, k = 1, \ldots, 20$). Note now that, due to the convexity of V_3 we have that, for all k,

$$\sum_{j=1}^{5} V_3(\pi_j^k) \geq 5V_3 \left(\frac{1}{5} \left(\sum_{j=1}^{5} \pi_j^k \right) \right). \tag{34}$$

On the other hand, we have that

$$\frac{1}{5} \left(\sum_{j=1}^{5} \pi_j^k \right) \leq \frac{3}{5}\pi. \tag{35}$$

Indeed, the latter is a consequence of the fact that the internal angles of a 5-cycle sum up at most to 3π. In particular, we have equality if and only if the 5-cycle is planar. Hence, owing to (34) and the monotonicity of V_3 we get that

$$\sum_{j=1}^{5} V_3(\pi_j^k) \geq 5V_3\,(3\pi/5) \tag{36}$$

and we have equality if and only if we have equality in (35). Hence, we can compute that

$$\begin{aligned} \tilde{V} &= \frac{1}{2} \sum_{i,j} V_2(\tilde{\ell}_{ij}) + \frac{1}{2} \sum_{k=1}^{12} \sum_{j=1}^{5} V_3(\pi_j^k) + \frac{1}{2} \sum_{k=1}^{20} \sum_{j=1}^{6} V_3(h_j^k) \\ &\geq \frac{1}{2} \sum_{i,j} V_2(\ell_{ij}) + \frac{1}{2} \sum_{k=1}^{12} 5V_3\,(3\pi/5) = V \end{aligned}$$

since hexagonal angles and bond lengths can only improve in passing to V. In particular, we have equality in the latter if and only if all pentagons and hexagons are planar and regular. That is if and only if the perturbation is trivial. □

A specific trait of the latter proof is that it crucially uses the *planarity* of the faces. This restricts our argument to the *only two* fullerenes which present just planar faces, namely C_{20} and C_{60} [30]. This restriction sounds quite severe as fullerenes are believed to possibly exists for arbitrary (even) $20 \leq n \neq 22$ and in a variety of different *isomers*. In particular, the nonisomorphic closed carbon cages for $n \leq 84$ amount to 222509 [8]. The investigation for possible stability criteria of the few observed fullerenes within this wide family has of course triggered an intense research and it would be probably too naive to expect our simple variational technique (which is, once again, purely geometric) to be decisive in this matter. Let us however mention that the possible relevance of planarity of the faces with respect to stability has been recently emphasized [20].

Still, the two fullerenes included in our result are truly remarkable structures. C_{60} is the most common fullerene as it is generally the first one to form during clustering, probably due to its uniformly distributed strain energy [21]. As such, C_{60} clearly has a predominant role within the fullerene class. The fullerene C_{20} is expected to possibly show a variety of interesting properties including superconductivity. Note however that the production of C_{20} is very delicate [23].

Eventually, we remark that the stability result of Theorem 7.3 applies to all structures made of regular planar pentagons and planar hexagons, possibly also nonclosed. In particular, our argument confirms that graphene patches and planar ground states are strict local minimizers in three dimensions. Moreover, one obtains also the stability of *corrannulene*, an open carbon cage formed by a pentagon surrounded by five hexagons, as well as of other corannulene-based molecules.

7.2. **Other three-dimensional configurations.** We presently do not have a characterization of ground states of V in three-dimensions. Still, under assumption (3) we can readily exclude that ground states are patches of FCC or HCP lattices, namely the candidate ground states for two-body interactions $V = V_2$ [17, 12]. Indeed, in both these cases one easily checks that an internal atom has exactly twelve active bonds and *at least* eight bond angles of $\pi/3$ (depending on the lattice). Hence, by *removing* an internal atom the energy of the resulting configuration fulfills $V_{\rm new} < V_{\rm old} + 12 - 8V_3(\pi/3)$. Under assumption (3), $V_{\rm new} < V_{\rm old}$ and FCC or HCP patches are not ground states.

Besides nanotubes and fullerenes, other intrinsically three-dimensional crystalline carbon allotropes exist: *diamond* and *lonsdaleite*. These are characterized by the occurrence of four-bonded atoms with bond angles equal to the *tetrahedral angle* $\theta_\tau = 2\arctan(\sqrt{2})$ arising in connection with so-called sp^3-hybridized orbitals. The computation of V to the leading order for both diamond and lonsdaleite gives $V \sim (-2 + 6V_3(\theta_\tau))n$. In particular, if and only if $V_3(\theta_\tau) \leq 1/12$ (which is still compatible with assumptions (3)-(5), although, given v, it cannot be enforced by merely triggering the constant μ) some sufficiently large (and suitably shaped) collection of diamond or lonsdaleite crystals realize a smaller energy than the corresponding planar ground state. Hence, such ensembles may be used for contradicting planarity in the proof of Theorem 7.1 (although under an extra assumption).

The latter argument can be also localized: By assuming $V_3(\theta_\tau) > 2/3$ we can exclude that diamond and lonsdaleite are ground states in three dimensions. Indeed, in this case it would be energetically favorable to *remove* from a ground state any four bonded atom being the center of a regular tetrahedron. Note incidentally that surface tension effects are not negligible for small n: Letting for instance $n = 5$, the single tetrahedron has energy $V = -4 + 6V(\theta_\tau)$ which is strictly larger than the planar ground state energy $-[3 \cdot 5/2 - \sqrt{3 \cdot 5/2}] = -4$ which is, for instance, obtained with a single chain of four bonds.

We shall remark that our functional V is specifically tailored to the description of sp^2-hybridized bonds and, as such, it appears to be not well-suited for describing intrinsically three-dimensional situations such that of diamond and lonsdaleite. Indeed, let V_3 be strictly convex around θ_τ (as for the Stillinger-Weber potential). Hence, a tetrahedral configuration for $n = 5$ with unit bonds is stable if and only if the sum of the bond angles is locally maximal. It can be proved that this is not the case for the regular tetrahedron (which may however be checked to be stationary for V). This entails in particular that diamond and lonsdaleite are not local minimizers of V.

Acknowledgements

E.M. and U.S. acknowledge the partial support of the FP7-IDEAS-ERC-StG Grant # 200947 *BioSMA*. E.M. acknowledges partial support by a postdoctoral scholarship of the Fondation Mathématique Jacques Hadamard and the hospitality from Paris-sud University. U.S. is partially supported by the CNR-AVČR Grant *SmartMath*, the CNR-JSPS Grant *VarEvol*, and the Alexander von Humboldt Foundation. Moreover, the authors acknowledge the hospitality of the Mathematisches Forschungsinstitut Oberwolfach where part of this research was developed. Finally, some insightful remarks by Paolo Piovano on a previous version of the manuscript are gratefully acknowledged.

References

[1] M. Arroyo and T. Belytschko. An atomistic-based finite deformation membrane for single layer crystalline films, *J. Mech. Phys. Solids*, 50 (2002), 9:1941–1977.

[2] X. Blanc and C. Le Bris. Periodicity of the infinite-volume ground state of a one-dimensional quantum model, *Nonlinear Anal.*, 48 (2002), 6:791–803.

[3] A. Braides and M. Cicalese. Surface energies in nonconvex discrete systems, *Math. Models Methods Appl. Sci.*, 17 (2007), 7:985–1037.

[4] A. Braides, M. Solci, and E. Vitali. A derivation of linear elastic energies from pair-interaction atomistic systems, *Netw. Heterog. Media*, 2 (2007), 3:551–567.

[5] D. W. Brenner. Empirical potential for hydrocarbons for use in stimulating the chemical vapor deposition of diamond films, *Phys. Rev. B*, 42 (1990), 9458–9471.

[6] D. W. Brenner, O. A. Shenderova, J. A. Harrison, S. J. Stuart, B. Ni, and S. B. Sinnott. A second-generation reactive empitical bond order (REBO) potential energy expression for hydrocarbons. *J. Phys. Condens. Matter*, 14 (2002), 783–802.

[7] B. J. Cox and J. M. Hill. Exact and approximate geometric parameters for carbon nanotubes incorporating curvature, *Carbon*, 45 (2007), 1453–1462.

[8] S. M. Daugherty. *Independent sets and closed-shell independent sets of fullerenes.* Ph.D. Thesis, University of Victoria, 2009.

[9] M. S. Dresselhaus, G. Dresselhaus, and R. Saito. Physics of carbon nanotubes, *Carbon*, 33 (1995), 883–891.

[10] W. E and D. Li. On the crystallization of 2D hexagonal lattices, *Comm. Math. Phys.*, 286 (2009), 3:1099–1140.

[11] L. Flatley, M. Taylor, F. Theil, and A. Tarasov. Packing twelve spherical caps to maximize tangencies, *J. Comput. Appl. Math.* 254 (2013), 220–225.

[12] L. C. Flatley and F. Theil. Face-centered cubic crystallization of atomistic configurations. In preparation, 2013.

[13] G. Friesecke and F. Theil. Geometry optimization, Binding of molecules, to appear in Encyclopedia of Applied and Computational Mathematics (Springer 2013).

[14] J. Fröhlich and C. E. Pfister. Absence of crystalline ordering in two dimensions, *Comm. Math. Phys.*, 104 (1986), 697-700.

[15] C. S. Gardner and C. Radin. The infinite-volume ground state of the Lennard-Jones potential, *J. Stat. Phys.*, 20 (1979), 6:719–724.

[16] S. Grivopoulos. No crystallization to honeycomb or Kagomé in free space, *J. Phys. A: Math. Theor.*, 42 (2009), 115212.

[17] L. C. Harris. *Face-centered cubic structures in energy-minimizing atomistic configurations*, PhD Thesis, Warwick University, 2011

[18] G. C. Hamrick and C. Radin. The symmetry of ground states under perturbation, *J. Stat. Phys.*, 21 (1979), 5:601–607.

[19] R. Heitman and C. Radin. Ground states for sticky disks, *J. Stat. Phys.*, 22 (1980), 3:281287.

[20] A. R. Kamatgalimov and V. I. Kovalenko. Deformation and thermodynamic instability of a C_{84} fullerene cage, *Russ. J. Phys. Chem. A*, 84 (2010), 4L721–726.

[21] H. W. Kroto. The stability of the fullerenes C_n, with $n = 24, 28, 32, 36, 50, 60$ and 70, *Nature*, 329 (1987), 529-531.

[22] C. Le Bris, P.-L. Lions. From atoms to crystals: a mathematical journey, *Bull. AMS*, 42, 291-363.

[23] F. Lin, E. Sørensen, C. Kallin, and J. Berlinsky. C_{20}, the smallest fullerene, in *Handbook of Nanophysics: Clusters and Fullerenes* (K. D. Sattler, ed.), Taylor & Francis, CRC Press, 2010.

[24] A. Mielke. Private communication, 2012.

[25] S. Müller. Singular perturbations as a selection criterion for periodic minimizing sequences, *Calc. Var. Partial Differential Equations*, 1 (1993), 2:169–204.

[26] C. Radin. Classical ground states in one dimension, *J. Stat. Phys.*, 35 (1983), 1-2:109–117.

[27] C. Radin and L. S. Schulmann. Periodicity of classical ground states, *Phys. Rev. Lett.*, 51 (1983), 8:621–622.

[28] C. Radin. Low temperature and the origin of crystalline symmetry. *Int. J. Mod. Phys. B*, 1 (1987), 5-6:1157 1191.

[29] C. Radin. The ground state for soft disks, *J. Stat. Phys.*, 26 (1981), 2:365–373.

[30] S. Schein and T. Friedrich. A geometric constraint, the head-to-tail exclusion rule, may be the basis for the isolated-pentagon rule for fullerenes with more than 60 vertices. *Proc. Nat. Acad. Sci. U.S.A.*, 105 (2008), 19142–19147.

[31] B. Schmidt. Ground states of the 2D sticky disc model: fine properties and $N^{3/4}$ law for the deviation from the asymptotic Wulff shape. *J. Stat. Phys.*, (2013), to appear.

[32] F. H. Stillinger and T. A. Weber. Computer simulation of local order in condensed phases of silicon, *Phys. Rev. B*, 8 (1985), 5262–5271.

[33] J. Tersoff. New empirical approach for the structure and energy of covalent systems. *Phys. Rev. B*, 37 (1988), 6991–7000.

[34] F. Theil. A proof of crystallization in two dimensions, *Comm. Math. Phys.*, 262 (2006), 1:209–236.

[35] F. Theil. Suface energies in a two-dimensional mass-spring model for crystals, *ESAIM Math. Model. Numer. Anal.*, 45 (2011), 873–899.

[36] W. J. Ventevogel. On the configuration of a one-dimensional system of interacting particles with minimum potential energy per particle, *Phys. A.*, 92 (1978), 3-4:343–361.

[37] W. J. Ventevogel and B. R. A. Nijboer. On the configuration of systems of interacting particle with minimum potential energy per particle, *Phys. A.*, 98, (1979), 1-2:274–288.

[38] W. J. Ventevogel and B. R. A. Nijboer. On the configuration of systems of interacting particle with minimum potential energy per particle, *Phys. A.*, 99, (1979), 3:565–580.

[39] H. J. Wagner. Crystallinity in Two Dimensions: A Note on a Paper of C. Radin, *J. Stat. Phys.*, 33, (1983), 3:523-526,

[40] J. Wu, K. C. Hwang, Y. Huang. An atomistic-based finite-derformation shell theory for single-wall carbon nanotubes, *J. Math. Phys. Solids*, 56 (2008), 279–292.

[41] Y. A. Yeung, G. Friesecke, B. Schmidt. Minimizing atomic configurations of short range pair potentials in two dimensions: crystallization in the Wulff shape, *Calc. Var. Partial Differential Equations*, 44 (2012), 81–100.

(Edoardo Mainini) Università degli Studi di Genova, Dipartimento di Ingegneria meccanica, energetica, gestionale e dei trasporti (DIME) - sezione MAT, p.le Kennedy 1, 16129 Genova, Italy

(Ulisse Stefanelli) Istituto di Matematica Applicata e Tecnologie Informatiche "E. Magenes" - CNR, v. Ferrata 1, I-27100 Pavia, Italy, and Faculty of Mathematics, University of Vienna, Oskar-Morgenstern-Platz 1, A-1090 Vienna, Austria